

DYNAMICS OF SPONTANEOUS SPREADING WITH EVAPORATION FOR THIN SOLVENT FILMS

ANNE D. DUSSAUD and SANDRA M. TROIAN

Department of Chemical Engineering, Princeton University, Princeton NJ 08544-5263

ABSTRACT

We have investigated the spreading behavior of solvent droplets on a bulk water support using solvents with different vapor pressures and spreading coefficients. Instead of seeding the surface with tracer particles, as is usually done to track moving fronts, we employ laser shadowgraphy to visualize the entire surface of the spreading film including the leading edge. For non-volatile systems it has previously been shown that the leading edge advances in time as $t^{3/4}$. We find that volatile systems with positive initial spreading coefficients exhibit two spreading fronts, both of which demonstrate power law growth but with exponents closer to 1/2. Surprisingly, differences in the liquid vapor pressure or the spreading coefficient seem only to effect the speed of advance but not the value of the exponent. We are presently investigating the behavior of the subsurface flow to determine the mechanism leading to the smaller spreading exponent.

INTRODUCTION

Processes ranging from the casting of membranes from spread films to the advance of oil slicks during the late stages of a spill all require detailed knowledge of the spreading dynamics of solvent films along the surface of a bulk liquid support. Spontaneous spreading is generally ruled by the spreading coefficient, S , first defined by Harkins [1] to be $S = \gamma_1 - \gamma_2 - \gamma_{12}$ where γ_1 denotes the surface tension of the uncontaminated liquid or solid substrate, γ_2 the vapor/liquid surface tension, and γ_{12} the interfacial tension between the spreading film and the liquid or solid support. Spontaneous flow induced by variations in surface tension gives rise to Marangoni flow so-named after Carlo Marangoni, who first realized that the spreading coefficient determines whether a liquid will spread spontaneously over a supporting surface ($S \geq 0$) or remain in equilibrium with the support by assuming a lenticular shape ($S < 0$) [2]. Much of the work devoted to Marangoni spreading has focused almost exclusively on pure, immiscible and non-volatile surface films. In such cases, a simple scaling analysis proposed by Fay [3] outlines the scaling analysis which determines the location of the advancing front of the spreading film, $L(t)$. Assuming that the spreading film remains coherent from the source of deposition to the leading edge and that the thin spreading film undergo plug flow, a force balance at the film surface, $z = 0$, determines the position of the advancing front for both unidirectional or axisymmetric flow. Fay reasoned that the spreading coefficient reflects the net surface force per unit length, F_S , created by the Marangoni stress at the surface such that $F_S = \int_0^{L(t)} \frac{\partial \gamma}{\partial x} dx = S$. The viscous drag from the sublayer creates a surface shear stress per unit length $F_V = \int_0^{L(t)} \mu \left[\frac{\partial u}{\partial z} \right]_{z=0} dx$, where the coordinates x and z represent the horizontal and vertical directions, respectively. Estimating this viscous drag to be $\mu \frac{UL}{\delta}$ and substituting from boundary layer theory the surface velocity, $U = L/t$, and the boundary layer thickness $\delta = (\frac{\mu}{\rho} t)^{1/2}$, leads directly to the relation $L(t) = K \frac{S^{1/2}}{(\mu\rho)^{1/4}} t^{3/4}$. The subphase viscosity and density are denoted by μ and ρ . This relation determines the position of the

leading edge of a thin surface active film supplied from an infinite reservoir and spreading along a thick liquid support of higher tension under the action of Marangoni forces. Since there has been surprisingly little study of spreading phenomena in the presence of evaporation, we present a systematic experimental study of the spreading kinetics of several volatile but immiscible hydrocarbon films advancing over a bulk water support. We performed these studies to determine whether or not there exists some universal behavior that describes the advance of a spreading film undergoing evaporation. As we show below, there does appear to exist a power law advance with a smaller temporal exponent even for systems experiencing significant mass loss during spreading.

EXPERIMENT

Materials

In order to separate the effects due to the strength of the spreading coefficient and the effects due to vapor pressure of the spreading film, four immiscible solvents with significantly different volatilities and spreading coefficients were chosen to vary the range of spreading behaviors. The four solvents, used as received, were toluene (99.8%, Aldrich), p-xylene(99+, Aldrich), 2,2,4 trimethylpentane (99.9%, Aldrich) and n-heptane (spectrophotometric grade, Mallinckrodt). Pure silicone oil (1000 mPa.s, Fluka) was chosen as the control sample in our studies since previous work has shown that silicone oil spreading on water exhibits model Marangoni spreading with a 3/4 exponent and a coefficient that agrees well with theoretical predictions [4]. The physical and interfacial properties of these spreading fluids are presented in Table I. The supporting liquid was distilled and deionized ultra pure water ($18M\Omega \cdot cm^{-1}$).

Table I: Physical and interfacial properties of spreading solvents

Spreading liquid	Boiling point (°C)	Vapor pressure (mm Hg) 25° C	S ± 0.2 mN.m ⁻¹ 23° C
Toluene	110.6	30	8.2
p-Xylene	138.4	8.7	7.4
Trimethylpentane	99.2	49	4.1
Heptane	98.4	45.7	2.3
Silicone oil	-	0	9.4

Visualization Technique

The experiments were performed in a circular glass dish of 16 cm diameter and 8 cm depth fit specifically with an optically flat bottom. The oil spreading over the water surface was visualized by laser shadowgraphy, a method especially well suited to detecting surface deflections in liquid films. The glass cell is illuminated from below by a beam of monochromatic light from a 1 mW He-Ne laser. The beam is expanded by first passing through a spatial filter and then through a collimating lens to provide a uniformly lit area of 9 cm diameter with which to visualize a significant portion of the spreading film. Shadows created from any surface deflections are formed onto a projection screen of ground glass and recorded onto SVHS tapes by a high resolution CCD camera. The video images were analyzed to deduce the temporal advance of any regions of high curvature. The leading edge of the spreading film was detected by the presence of the well-known Thoreau-Reynolds ridge as observed by

McCutchen [5] and Scott [6] who studied in detail the spreading of non-volatile organic films on water. This ridge is produced by the very high surface shear stress at the leading edge of the boundary layer and corresponds to the variable $L(t)$ introduced above.

Procedure

All parts in contact with the liquids were carefully cleaned using solvents and sulfochromic acid and rinsed with copious amounts of distilled water. The cell was filled with ultrapure water to a depth of 3 cm. During the experiment the cell remained completely open to the atmosphere to provide fully unsaturated conditions for the solvent vapor in order to maximize evaporation from the spreading film. A small and precise volume ($2-4 \mu\text{l}$) of solvent was carefully deposited onto the pure water surface. One droplet was deposited every 40 seconds, a time period during which we determined the solvent film completely evaporates from the water surface, thereby returning the water to its original high surface tension value (see Ref. 7 for more details). Three runs of ten successive depositions were performed for each solvent.

RESULTS

Since laser shadowgraphy has not previously been used to visualize spreading rates of thin films, we tested our apparatus by studying the leading edge of silicone oil spreading on a water film. A typical shadowgraph of the spreading of a silicone oil droplet is shown Fig.1a along with a sketch of the surface profile in Fig.1c. The outside bright ring, denoted by L, is used to track the propagation of the leading edge, $L(t)$, as plotted in Fig. 2. The bright ring in the inner region, denoted by R, corresponds to the periphery of the droplet reservoir that feeds the advancing film. As shown in Fig. 2, the data for $L(t)$ for the silicone oil, which

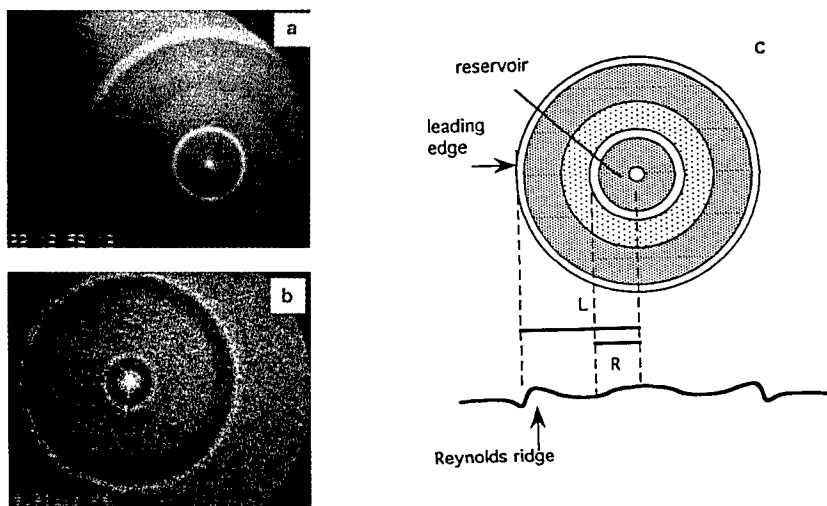


Figure 1 : Typical shadowgraph of the spreading of silicone oil (a) and toluene (b) at $t=0.30$ s. (c) Sketch of the surface profile corresponding to a shadowgraph.

neither evaporates nor dissolves in water, allows a fit to a power law with an exponent of 0.74, in excellent agreement with the theoretical value of $3/4$. We note that these control experiments with silicone oil establish that in spite of the small range of available observation times for the spreading dynamics, the temporal advance of the spreading film is well characterized by the appropriate power law. As shown in Fig. 1b, the surface spreading profiles of the solvent films appear similar to the spreading of silicone oil. We detect, however, two fronts of high curvature corresponding to the leading edge and to the periphery of the droplet reservoir. We have observed that after this initial spreading regime which lasts on order of 1.5 sec, the reservoir edge R stops growing and achieves a plateau in time. At this point the reservoir becomes unstable and undergoes a peculiar dewetting instability followed by a period of turbulent mixing and retraction [8]. We are presently studying this instability in order to determine the mechanism for film rupture and recession. We have only presented here results from the initial stage of spreading, $t \leq 2$ sec, during which the reservoir is well behaved and stable.

The evolution of $L(t)$ for the solvents toluene, xylene, heptane and trimethylpentane is shown Fig. 2.

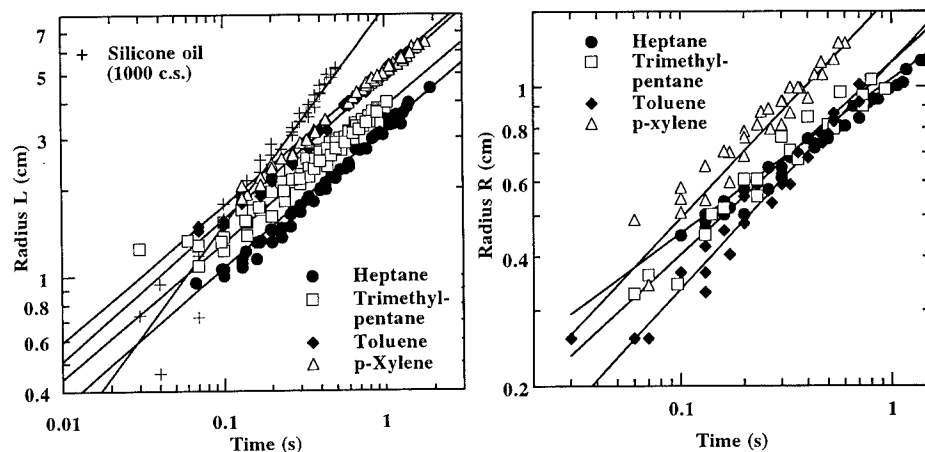


Figure 2: Radius of leading edge $L(t)$ Figure 3: Radius of reservoir edge $R(t)$

Table II shows the results of power law fits to the data with k and α as adjustable parameters. Each entry represents the average over N independent spreading events. The standard deviation for the location of the advancing fronts for each solvent tested is approximately $\pm 8\%$ indicating good reproducibility between runs. As seen from the values in Table II, the spreading exponent for the leading edge is approximately $1/2$, irrespective of the solvent used. This value is significantly lower than the $3/4$ value observed for the spreading of non-volatile and immiscible surface films. To determine the dependence of k on some spreading parameters, we plot in Fig. 4 the value of k vs. the spreading coefficient S . Clearly the speed of propagation of the leading edge increases with S . This suggests that the spreading of the front is driven by Marangoni forces. The experimental values for k seem approximated by the empirical relation $k \simeq S^{0.36}$. Several other volatile solvents with a wider range of spreading coefficients must necessarily be tested to confirm this tendency.

Table II: Results of fitting data to the form $\bar{r} = kt^\alpha$. \bar{r} denotes the spreading distance, α the spreading exponent, and k the overall coefficient. N is the number of droplets deposited in total on one surface, and r , the mean value of the linear correlation coefficient.

Solvent	Leading edge L				Reservoir R			
	N	α	k	r	N	α	k	r
Toluene	10	0.49± 0.05	4.86± 0.27	0.9986	20	0.53± 0.05	1.14± 0.10	0.9935
Xylene	10	0.47± 0.02	5.15± 0.16	0.9986	20	0.52± 0.05	1.63± 0.13	0.9904
Trimethyl - pentane	10	0.47± 0.03	3.83± 0.15	0.9972	11	0.45± 0.03	1.14± 0.11	0.9908
Heptane	13	0.48± 0.04	3.22± 0.11	0.9925	13	0.36± 0.02	1.04± 0.07	0.9963

In particular, it remains unclear whether xylene and toluene propagate at the same speed since although their spreading coefficients are very close, their vapor pressures are fairly different. The time evolution of the reservoir periphery $R(t)$ is plotted in Fig. 3. The reservoir spreads 3 to 4 times more slowly than the leading edge. The data were fitted by a power law with an exponent ranging between 0.35 and 0.53. The coefficient for the reservoir periphery k vs. S is not described by a power law in contrast to the behavior of the leading edge shown in Fig. 3. The reservoir spreading seems affected by the volatility of the spreading material. Indeed, the reservoirs of the three solvents, toluene, trimethylpentane and heptane, which have rather similar vapor pressures, spread almost all at the same speed. The reservoir for xylene, which is the least volatile solvent, spreads significantly more rapidly.

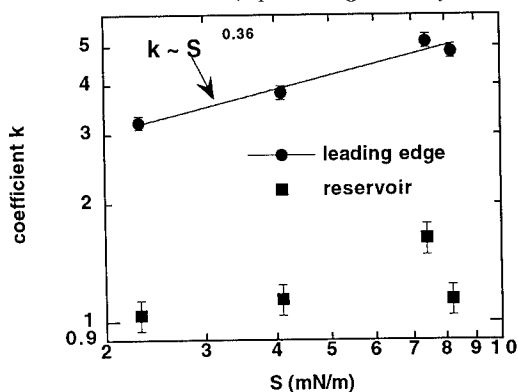


Figure 4: Coefficient k versus the spreading coefficient.

It can easily be shown that if the reservoir spreading is driven by the balance of capillary and viscous forces, then the reservoir advances with an exponent of $3/4(2 + \alpha)$ for rectilinear ($\alpha = 1$) or axisymmetric geometry ($\alpha = 2$) [7]. Surprisingly, the velocities as well as the exponents we obtained (0.35-0.53) are all higher than the values typically attained by capillary driven spreading on a thick liquid support indicating the dominant effect of Marangoni forces.

CONCLUSIONS

In lieu of the usual technique of surface tracer particles which can only track an advancing liquid front, we have used laser shadowgraphy to monitor the entire spreading profile of thin immiscible volatile films spreading along the surface of a bulk water support. Because the volatile films have a surface tension lower than that of pure water, the films spread spontaneously and rapidly under the action of Marangoni forces. Using different volatile solvents, we have uncovered that the leading edge exhibits a spreading behavior well characterized by the relation $L(t) = kt^\alpha$ with $\alpha \approx 1/2$, irrespective of the spreading coefficient or vapor pressure of the volatile liquid used. The coefficient k appears to increase with the value of the spreading coefficient S . There also appears power law growth in a second advancing front associated with the reservoir droplet periphery, though the speed of advance in this regime appears controlled by the volatility of the liquid studied. We are presently characterizing a mechanism which may be responsible for the decrease in exponent of the leading edge from $3/4$ to approximately $1/2$ associated with a subsurface instability created by the significant surface cooling induced by the rapid spreading [7]. There appears to develop a Bénard-like cellular roll under the Thoreau-Reynolds ridge which systematically slows the advance of the spreading film. A discussion of this aspect of the flow as well as some scaling suggestions to determine the $1/2$ exponent can be found in the upcoming publication in Ref. 7. We hope these and similar studies can help improve present forecasting models for the areal coverage of a contaminant spill when only Marangoni and viscous forces determine the extent of spreading.

ACKNOWLEDGMENTS

We gratefully acknowledge support from the Ministère Français de la Recherche for a post-doctoral fellowship (ADD) as well as an NSF CAREER Award (SMT).

REFERENCES

1. W. D. Harkins in The Physical Chemistry of Surface Films, Reinhold Publishing. Corp., New York (1952).
2. C.G.M. Marangoni, *Nuovo Cim.* **2**, p. 239, (1872).
3. J.A. Fay in Oil on the sea edited by D. Hoult, Plenum Press, New York (1969).
4. D.W. Camp and J. C. Berg, *J. Fluid Mech.* **184**, p. 445, (1987).
5. C.W. McCutchen, *Science* **170**, p. 61, (1970).
6. J. C. Scott, *J. Fluid Mech.* **116**, p. 283, (1982).
7. A.D. Dussaud and S.M. Troian, submitted to *Phys. Fluids*.
8. S.M. Troian and J. M. Drake, in preparation.